Solar Energetic Particle Events in Different Types of Solar Wind

S. W. Kahler
Air Force Research Laboratory, Space Vehicles Directorate, 3550 Aberdeen Ave., Kirtland AFB, NM 87117, USA
stephen.kahler@kirtland.af.mil
and

A. Vourlidas
Space Sciences Division, Naval Research Laboratory, Washington, DC 20375, USA

ABSTRACT

We examine statistically some properties of 96 20-MeV gradual solar energetic proton (SEP) events as a function of three different types of solar winds (SWs) as classified by Richardson and Cane (2012). Gradual SEP ($E > 10$ MeV) events are produced in shocks driven by fast ($V \gtrsim$ 900 km/s) and wide ($W > 60°$) coronal mass ejections (CMEs). We find no differences between transient and fast or slow SW streams for SEP 20-MeV event timescales. It has recently been found that the peak intensities Ip of these SEP events scale with the $\sim$ 2-MeV proton background intensities, which may be a proxy for the near-Sun shock seed particles. Both the intensities Ip and their 2-MeV backgrounds are significantly enhanced in transient SW compared to those of fast and slow SW streams, and the values of Ip normalized to the 2-MeV backgrounds only weakly correlate with CME V for all SW types. This result implies that forecasts of SEP events could be improved by monitoring both the Sun and the local SW stream properties and that the well known power-law size distributions of Ip may differ between transient and long-lived SW streams. We interpret an observed correlation between CME V and the 2-MeV background for SEP events in transient SW as a manifestation of enhanced solar activity.

Subject headings: acceleration of particles—Sun: flares—Sun: particle emission—Sun: coronal mass ejections (CMEs)

1. INTRODUCTION

The good association of $E > 10$ MeV SEP events with energetic coronal mass ejections (CMEs) is attributed to diffusive shock acceleration near the Sun of a population of seed particles, which may have suprathermal energies (Tylka and Lee 2006). The shock is driven by the CME, but the timing and location of the particle-acceleration regions of the shock, the transport of the particles to magnetic field lines connecting to an observer, and a characterization of the seed population are all subjects of current study. These phenomena are not directly observed, so even when a large eruptive solar event occurs, the forecasting of SEP events, a basic component of space weather, is a refractory problem.

A basic consideration is that the Alfvén V_A and solar wind (SW) Vsw speeds (Kahler 2004) and the abundances of suprathermal ($Vp \gtrsim 2 \times Vsw$, where Vp is the particle speed) particles (Gloeckler 2003) are known to vary with the type of SW, such that one would expect more frequent or energetic SEP events in slow rather than in fast SW regions (Kahler and Reames, 2003). Transient SW regions, associated with interplanetary CMEs (ICMEs) constitute a third type of SW, often differing from slow and fast SW in their thermal or suprathermal particle compositions (Zurbuchen & Richardson 2006, Mewaldt et al. 2007, Reinard et al. 2012, Gruesbeck et al. 2012) and V_A speeds.

Using a variety of in-situ particle and field observations, Richardson and Cane (2012, hereafter CR12) have classified the SW over the period 1963 to 2011 into three types. Type 1 is transient flows (Zurbuchen and Richardson 2006) originating with CMEs and including upstream shock/sheath regions as well as associated disturbed regions following ICMEs. Type 2 is the co-rotating high-speed streams, and type 3 is the interstream, or slow, SW. Several studies of SEP event properties have been based on updated versions of their background SW list. A search for variations in SEP event timescales TO (time from CME launch to SEP onset) and TR (time from SEP onset to half the maximum intensity) of SEP events observed from 1998 to 2002 showed no dependence on SW type, except for a slight trend of smaller TO within the transient streams (Kahler 2005, 2008). Kahler et al. (2014) recently found a similar result for a different set of 41 SEP events originating from within 20° of central meridian.

A survey by Kahler et al. (2009) of SEP-event elemental abundance variations by CR12 SW type found that despite the large ranges in abundance ratios of Mg/Ne, Fe/O, C/O, and He/H at 5–10 Mev nucleon^{-1}, no differences among SW types were found. On the other hand, sorting time-averaged intensities of 227 SEP events, Kahler et al. (2009) found that 2 and 20 MeV H and 5–10 MeV nucleon^{-1} Fe, Ne, C, and Mg intensities were about an order of magnitude larger in the transient type 1 SW compared with those of SW types 2 and 3. A similar enhancement appeared in the peak intensities Ip of the 41 20-MeV SEP events of Kahler et al. (2014). Fifteen of those were in transient SW streams, of which 8 were magnetic clouds (MCs, Gulisano et al. 2012), and three of those 8 SEP events were ground level events (GLEs).

The organization of differential size distribution of SEP events into a power law of Ip with exponent $\alpha_p = -(1.2\text{–}1.4)$ has long been known (Belov et al. 2007, Cliver et al. 2012). However, the supporting SEP observations have been accumulated over all three SW types without distinguishing the SEP event distributions in each type. If those SEP size distributions differ by SW type, then attempts to understand SEP origins and to relate SEP events to associated solar-flare size distributions (Cliver et al. 2012) may need reconsideration.

We have recently used a set of 96 20-MeV proton events, first to characterize the energetics of SEP events and their associated CMEs (Kahler and Vourlidas 2013), and then to compare SEP events for which the primary CME driving the shock was or was not preceded by one or more preCMEs meeting several criteria (Kahler and Vourlidas 2014). In the latter study we found a good correlation between the 20-MeV event Ip and the 2-MeV proton background intensities. We also found a correlation between the 2-MeV background intensity and the occurrence of preCMEs, which we interpreted as a manifestation of enhanced solar activity. Thus, the correlations of SEP event Ip with both 2-MeV proton backgrounds and occurrences of preCMEs left uncertain which of the two phenomena might be the more important or perhaps only causal factor leading to the enhanced SEP event intensities Ip. We favored the 2-MeV proton backgrounds, but our analysis using 2-MeV proton backgrounds with SEP event data from the two studies (Gopalswamy et al. 2004, Ding et al. 2013) supporting preCMEs as the physically important factor did not confirm our finding of a correlation of SEP Ip with the backgrounds.

In this work we use the same 96 20-MeV SEP events to examine again the question of whether SW type plays any role in the timescales or Ip of SEP events. Based on our previous results (Kahler & Vourlidas 2013, 2014), we also include the 2-MeV backgrounds as part of the analysis. In the following sections we discuss the data selection and analysis.

2. DATA ANALYSIS

2.1. Event Selection and Criteria

For this work we use the 20-MeV proton events observed with the EPACT/*Wind* detector over solar cycle 23 compiled by Kahler & Vourlidas (2013) in their study of associated CME dynamics. There were 96 SEP events with sources > W40° for which not only the CME properties could be calculated from *SOHO*/LASCO observations, but also 2-MeV proton event profiles were observable above background. For each SEP event the timescales TO and TR, defined above, and peak intensities Ip were taken from the event catalog of Kahler (2013). The pre-event 2-MeV proton backgrounds were measured separately as part of the analysis of Kahler & Vourlidas (2013).

We again use the updated CR12 SW list (Richardson 2013) to select the SW type present at the time of the SEP onset of each of the 96 SEP events. This yields a distribution of 34 type 1, 28 type 2, and 34 type 3 cases. We will sometimes combine types 2 and 3 into a total of 62 long-lived streams to compare with the 34 type 1 transients. We further divided the type 1 periods into three groups based on the ICME list maintained at the Advanced Composition Explorer (ACE) website http://www.srl.caltech.edu/ACE/ASC/DATA /level3/icmetable2.htm by Richardson and Cane (2010). Their list classifies ICMEs into three groups: 0, not a magnetic cloud (MC) and lacking typical MC features; 1, rotation of field direction but lacking other MC features; and 2, MCs. For our analysis we call their groups 0 and 1 QuasiMCs and any type 1 periods not on the ICME list simply as Other. We will refer to all type 1 periods as transients.

Two CME speeds are given in Table 1, the linear speed V(cdaw) given in the CDAW catalog and the V(fr) frontal speeds measured for the analysis of Kahler & Vourlidas (2013). Their comparison of the two CME speeds for 37 selected cases showed a good correlation coefficient of CC = 0.93. The CME widths are taken from the CDAW catalog. We compute median values for most of the parameters of the study to compensate for their broad distributions, which are characterized by high formal standard deviation values, and present the values in Table 1. Correlations between parameter pairs are given in Table 2.

2.2. SEP Event Timescales in SW Types

The median values of TO, TR, and TO+TR for the three SW types are given in the second to fourth rows of Table 1. The parameter TO+TR is not affected by the SEP background intensity and is a more robust parameter than either TO or TR (Kahler 2013). The values in all SW types are comparable to those in the W33°–WL longitude range of Table 3 of Kahler (2013), of which they are a subset. The timescales are all slightly larger in the SW 1 transients than in the combined SW 2+3 streams, but the standard deviations greatly exceed the differences, so we conclude that there are no significant differences in the SEP event timescales among the three SW stream types or between the SW type 1 and the long-lived SW types 2+3..

2.3. SEP Event Peak Intensities in SW Types

The fifth line of Table 1 gives the median values of the logs of the peak 20-MeV intensities Ip for the different SW types. The transient type 1 median is a factor of 10 higher than those of the types 2 or 3 or 2+3. That difference is less than the standard deviation of the entire distribution, which results from the few large events in the distribution. In Figure 1 we compare the numbers of 20-MeV SEP events in bins of logs of the differential Ip for the stream and transient SW types. Those in the transients form a flatter distribution and dominate the two decades of highest peak differential Ip.

We find the expected correlation between logs of the 20-MeV Ip and the CME V(cdaw) for all SW types, but the correlation in SW type 1 is much higher than for types 2 or 3 or the combined 2+3, as indicated in the second line of Table 2. As a rough guide for the SW groups of size ∼32 events, a CC = 0.45 is significant at the 99% level (Bevington and Robinson 2003). Figure 2 shows the considerable overlap and large scatter in log values of both Ip and V(cdaw) and the somewhat higher values of V(cdaw) for the SW type 1 events compared to those of types 2 and 3. Very similar results are obtained for the median CME V(fr) speeds (Table 1).

The results of our previous work on SEP events and preCMEs (Kahler & Vourlidas 2014) suggest an important role for the low-energy 2-MeV proton backgrounds. We see in Table 1 that those type 1 background intensities are also enhanced over those of types 2 and 3 and in the first line of Table 2 that they are strongly correlated with 20-MeV Ip in all SW types. To try to separate the effects of the 2-MeV backgrounds from those of the CME speeds on the SEP Ip values, we first normalize Ip to the 2-MeV background by forming the ratios R1 = Log(Ip/bkgd). The R1 values are now only weakly correlated with log V(cdaw) as shown in Table 2 and Figure 3.

We might understand within the diffusive shock scenario that Ip should increase with faster CMEs and shocks and with higher intensities of low-energy seed particles, but we find in addition that the 2-MeV proton background intensities themselves strongly correlate at $> 99.9\%$ significance with the CME speeds for the SEP events in SW type 1. This result is presented in the last line of Table 2 and in Figure 4. There is no significant correlation for SW types 2 and 3. The last two lines of Table 1 show that the CMEs associated with the SW type 1 SEP events are also slightly wider and tend to occur closer to solar central meridian than those of types 2 and 3.

2.4. SEP Events in Transient SW

The results of the previous sections indicate an enhancement in SW type 1 not only of the SEP Ip, but of 2-MeV backgrounds, as well as CME speeds and widths. We can look further into the 34 SW transients by separately comparing properties of the three type 1 groups described in Section 2.1: 8 MCs, 10 QuasiMCs, and 16 Other. The median properties for this small set of SEP events is given in Table 3. The only outstanding differences among the three group medians are the lower Ip values for the MCs, which appear to result from the lower associated V(cdaw) values and 2-MeV backgrounds, as shown in Figure 5. The dates of the two largest MC events are 21 April 2002 and 10 November 2004.

2.5. SEP Event Selection and Power-Law Size Distributions

The SEP event size-number distribution of Figure 1 is plotted on a linear-log plot rather than a log-log plot as one might expect from the power-law distributions derived for SEP event peak intensities Ip (Belov et al. 2007, Cliver et al. 2012). For 1265 SEP events over the period 1975–2005 Belov et al. (2007) derived a power-law exponent of $\alpha_p = -1.22$ for proton events with $E > 10$ MeV over more than five orders of magnitude. If we had selected SEP events randomly by size, then our distribution might resemble the steep power-law distribution shown in the central part of Figure 6, which decreases by a factor of 16.6 for each decade. We find, however, that not only our selection of SEP events, but also those of Gopalswamy et al. (2004), Cliver et al. (2012), and Ding et al. (2013) have size distributions sufficiently flat to plot them on the linear-log scale of Figure 6. We converted our $E = 20$-MeV Ip values of differential intensities to the equivalent integral $E > 10$-MeV Ip values of the other three studies by assuming an energy power-law exponent of $\gamma = 2.5$ (Kahler 2001). Also note that the low-intensity selection thresholds differed among the studies shown.

It is clear that SEP event selection criteria, in particular good solar magnetic connections and CME and flare associations, introduce a strong bias toward more intense SEP events. The statistical compilations of SEP event peak intensities (e.g., Cliver et al. 2012) have not distinguished among SW types since there was no reason to look for such differences. If those SEP event size distributions were compiled separately by SW type, as we have done here, then we might expect a significantly flatter size distribution for those events in the transient SW, similar to events of Figure 1. This could be done by comparing the 222 $E > 10$ MeV SEP events with well connected solar sources at W20°–W75° of Belov et al. (2007) with the SW types over the same period (Richardson & Cane 2012). The difference in size distributions may shrink or disappear when solar events from poorly connected sources are considered.

3. DISCUSSION

3.1. Comparisons with Earlier Work and SEP Forecasting

The primary result of this work is that the intensities Ip of the 20-MeV SEP events are statistically larger in transient SW than in the long-lived fast and slow SW by about an order of magnitude (Table 1). This large difference is still less than the computed standard deviation, although Figures 1 and 2 make clear that the Ip values are far from Gaussian in distribution. This result was based on 96 20-MeV SEP events with associated CMEs and solar source regions at longitudes > W40° and supports two similar earlier findings of enhanced SEP events using different SEP-event properties. The first result (Kahler et al. 2009) used 227 SEP events from all solar longitudes selected independently of CME associations and divided into 325 time segments, of which 128 lay in transient SW. The SEPs consisted of 2 and 20 MeV protons and 5–10 MeV nucleon^{-1} C, Ne, Mg, and Fe. The second (Kahler et al. 2014) used 20-MeV proton events with solar source regions within 20° of solar central meridian. Their Figure 3 shows that the median intensity Ip in the 15 SW transients was more than a standard deviation above that of the 26 long-lived SW streams. While the SEP events differ in these three studies, all SW types are based on the classification list of Richardson (2013).

Miteva et al. (2013) carried out a similar statistical study to compare properties of SEP events in ICMEs with those in quiet SW (their SoWi) and found no difference in intensities between their two groups. However, their SEP events were those with sources 0° to $<90^\circ$ from the catalog of Cane et al. (2010), and their ICME periods were only those in the ACE catalog (Richardson & Cane 2010), which correspond to our 8 MC and 10 QuasiMC events of Table 3. For those 18 SEP events we find a median log 20-MeV p Ip of −1.67, comparable to the median of −1.52 for the SW 2+3 type of Table 1. Miteva et al. (2013) also found that the SEP rise times are about a factor of 3 smaller in ICMEs than in their SoWi group (their Figure 2). Their rise times are defined in terms of an exponential rise within a limited intensity range, only roughly comparable to our TR times, for which we find larger medians in the SW type 1 than in type 2+3. To summarize this comparison of the two studies, we may have incompatible results for TR, but not for the log 20 MeV p Ip intensities, keeping in mind the several differences of event selections and treatment.

Since one can generally determine from either current 1-AU observations or model forecasts the SW type at the time of an expected SEP event, a forecast model for SEP intensities Ip could be modified to reflect the distributions of Ip shown in Figure 1. The background energetic ($\sim$ 0.1–100 MeV) particle intensities are one signature of transient SW (Richardson and Cane 2012), but the $\sim$ 2-MeV proton background intensities may be of further use in terms of forecasting intensities Ip. Ip is strongly correlated with CME V(cdaw) (Table 2), but V(cdaw) is difficult to determine in real-time coronagraph observations. Log Ip correlates about as well with log 2-MeV background as with CME V(cdaw), so a better approach might be to attempt a forecast of the ratio R1, which is less correlated with or dependent on V(cdaw), as shown in Table 2 and Figure 3. A caveat here is that our result is based only on SEP events with sources $>$ W40°, so the derived correlations may be very different for SEP events with origins near disk center or in the eastern hemisphere.

3.2. 2-MeV Protons at 1 AU and Near the Sun

We have normalized the peak 20-MeV SEP intensities Ip with the 2-MeV p backgrounds measured at 1 AU just prior to the SEP event onsets. The motivation was to use a 1-AU signature of the low-energy seed particle population of the CME-driven shock near the Sun. The travel time for 2-MeV protons to traverse the Parker spiral to 1 AU is 2.5 hours, so any substantial change in the near-solar proton intensities will not be reflected at 1 AU before that time. Other studies have used low-energy ($\lesssim$ 1 MeV nucleon^{-1}) particle intensities observed a day before associated SEP event onsets (Mewaldt et al. 2012b, Ding et al. 2013) to allow for such changes to be observed at 1 AU. Those observations, however, are made in SW regions that will have rotated beyond Earth at the time of the following SEP event onset and may not match conditions in the solar regions magnetically connected to Earth at the time of event onset.

If cross-field proton propagation is faster than field-aligned propagation, then the earlier measurements would be more appropriate to allow time for 2-MeV protons to reach 1 AU. We take the contrary view that field-aligned particle propagation is faster (Giacalone 2010, Kelly et al. 2012, Reames 2013), and that observations in the same SW region as the SEP event, i.e., close to the event onset, better reflect the near-Sun seed population. The point may be moot, however, since particle transport may be dominated by substantial magnetic field-line wandering across the Parker spiral field (Ragot 2011, 2012; Giacalone & Jokipii 2012, Laitinen et al. 2013), and the low-energy particle intensities usually vary on timescales of hours or more. For a comparison, our version of Figure 4 of Ding et al. (2013), replacing their 1-day earlier daily average with a 2-hour average just before SEP onset, shows very similar distributions of peak SEP event intensities versus backgrounds for events with and without preCMEs.

3.3. 2-MeV Protons as Suprathermal Ions

Recent work (Desai et al. 2006b,c, Mewaldt et al. 2006, 2012b) indicates that the shock seed population for SEP events consists of suprathermal ($\gtrsim$ 10 keV nucleon^{-1}) rather than SW ions (Mason et al. 2005, 2013; Mewaldt et al. 2007). The suprathermal ion spectrum extends to $\sim$ 1 MeV nucleon^{-1} and has been observed in quiet SW and co-rotating interaction regions and from 1 AU on ACE to 5 AU on Ulysses (Gloeckler 2003, Gloeckler et al. 2008). It may be produced in shocks (Giacalone and Jokipii 2012) and impulsive and gradual SEP events and other processes (Desai et al. 2006a,c, Mason and Gloeckler 2012, Mewaldt et al. 2012a). The suprathermal ion intensities vary over 4 to 5 orders of magnitude, much more than those of the SW ions (Mason et al. 2005, Mewaldt et al. 2012b), and appear to limit the intensities Ip of associated SEP events (Mewaldt et al. 2012b) for which they are the seed population.

The suprathermal energy range is usually considered to be $\sim$2–30 $\times$ the SW speed (Mason and Gloeckler 2012), but the 2-MeV protons of our backgrounds extend to $\sim$ 40 $\times$ a SW speed of 400 km sec^{-1}. However, the 2-MeV background protons of this study lie near the suprathermal spectral rollover energy (Gloeckler et al. 2008) found for various ion species (Mason and Gloeckler 2012), so their role as seed particles can explain the good correlation of the 20-MeV SEP Ip with the 2-MeV backgrounds found in this work (Table 2) and in Kahler and Vourlidas (2014). Consequently, as suggested above, the 2-MeV proton background could be a good SEP forecasting tool. Mewaldt et al. (2012b) have also suggested that monitoring suprathermal (0.04–1.8 MeV nucleon^{-1}) particles at 1 AU could contribute to forecasting of SEP events.

3.4. SEP Size Distributions

The SEP/CME relationship for events in transient SW differs considerably from that in the slow and high-speed SW. The CME speeds are higher (Figure 2) and correlated with the presumed seed particle backgrounds (Figure 4). We attribute this unexpected result to a general enhancement of solar activity, which favors both faster CMEs, which tend to cluster in time (Ruzmaikin et al. 2011), as well as processes, not necessarily shock acceleration, leading to the higher SEP seed particle populations. There is a further implication that the size distribution of SEP event peaks, which is significantly flatter than that of solar X-ray flares (Cliver et al. 2012), may in fact be steeper in the long-lived SW streams than in the transient SW (Figure 6). If confirmed with a larger statistical study, this could have a bearing on the fundamental origin of SEP events.

The variation of Ip with SW type could also play havoc with attempts to determine the longitudinal distributions of SEP event intensities. Our measurements consist of single values of Ip for each event, separated by SW type as shown in Figure 1. We do not know how the SEP distributions vary across different stream types, but we might expect that comparisons of SEP intensities made at different longitudes for a given SEP event (Lario et al. 2013), but in different SW types, might give a misleading view of those spatial distributions. With the STEREO mission now providing widely separated observations for a number of SEP events (Dresing et al. 2012), it would be useful not only to test our result of enhanced Ip in transient SW, but to see whether the stream types affect the inferred longitudinal distributions (Mewaldt et al. 2013).

4. SUMMARY

The characteristics of SEP events as a function of the type of ambient SW in which they occur has been previously examined only in limited studies. We have compared a set of 96 20-MeV SEP events selected for good CME associations and limited to source longitudes > W40° in combination with an extensive list of all SW periods classified into three types. We have not found any difference in the event onset TO and rise TR timescales, but the transient SW is distinguished by median SEP intensities Ip an order of magnitude above those of the fast and slow SW. In all SW types the expected correlation of Ip with CME V(cdaw) is found, but when Ip is normalized to the background 2-MeV intensities, the normalized peaks are only weakly correlated with V(cdaw), suggesting that at least in the SEP events in transient SW the 2-MeV backgrounds indicate an abundance of shock seed particles needed for the production of the 20-MeV SEP event. The 2-MeV or lower-energy ion backgrounds at 1 AU may therefore serve as one component of a SEP forecasting system. The well known power-law size distributions of SEP events may be flatter in transient SW than in fast or slow SW, and this could be a problem for inferring longitudinal distributions of SEP event intensities.

S. Kahler was funded by AFOSR Task 2301RDZ4. A. Vourlidas was supported by the NASA LWS TR&T program. CME data were taken from the CDAW LASCO catalog. This CME catalog is generated and maintained at the CDAW Data Center by NASA and The Catholic University of America in cooperation with the Naval Research Laboratory. SOHO is a project of international cooperation between ESA and NASA. We thank D. Reames for the use of the EPACT proton data and I. Richardson for the use of his list of SW stream types.

REFERENCES

Belov, A., Kurt, V., Mavromichalaki, H., Gerontidou, M. 2007, Sol. Phys., 246, 457

Bevington, P. R., & Robinson, D. K. 2003, Data Reduction and Error Analysis for the Physical Sciences, McGraw Hill, New York

Cane, H. V., Richardson, I. G., & von Rosenvinge, T. T. 2010, J. Geophys. Res., 115, A08101

Cliver, E. W., Ling, A. G., Belov, A., & Yashiro, S. 2012, ApJ, 756, L29

Desai, M. I., Mason, G. M., Mazur, J. E., & Dwyer, J. R. 2006a, ApJ, 645, L81

Desai, M. I., Mason, G. M., Gold, R. E., Krimigis, S. M., Cohen, C. M. S., Mewaldt, R. A., Mazur, J. E., & Dwyer, J. R. 2006b, ApJ, 649, 470

Desai, M. I., Mason, G. M., Mazur, J. E., & Dwyer, J. R. 2006c, Space Sci. Rev., 124, 261

Ding, L., Jiang, Y., Zhao, L., & Li, G. 2013, ApJ, 763, 30

Dresing, N., Gómez-Herrero, Klassen, A., Heber, B., Kartavykh, Y., & Dröge, W. 2012, Sol. Phys., 281, 281

Giacalone, J. 2010, in Heliophysics: Space Storms and Radiation: Causes and Effects, ed. C. Schrijver & G. Siscoe, Cambridge U. Press, 233

Giacalone, J., & Jokipii, J. R. 2012, ApJ, 751, L33

Gloeckler, G. 2003, in AIP Conf. Proc. 679, Tenth Int. Solar Wind Conf., ed. M. Velli, R. Bruno, F. Malara, & B. Bucci (Melville, NY: AIP), 583

Gloeckler, G., Fisk, L. A., Mason, G. M., & Hill, M. E. 2008, in AIP CP1039, 7th Ann. Astrophys. Conf., eds G. Li et al., 367

Gopalswamy, N., Yashiro, S., Krucker, S., Stenborg, G., & Howard, R. A. 2004, J. Geophys. Res., 109, A12105

Gruesbeck, J. R., Lepri, S. T., & Zurbuchen, T. H. 2012, ApJ, 760:141

Gulisano, A. M., Demoulin, P., Dasso, S., & Rodriguez, L. 2012, A&A, 543, A107

Kahler, S. W. 2001, J. Geophys. Res., 106, 20947

Kahler, S. W. 2004, ApJ, 603, 330

Kahler, S. W. 2005, ApJ, 628, 1014

Kahler, S. W. 2008, Proc. 30th Int. Cosmic Ray Conf., 1, 143

Kahler, S. W. 2013, ApJ, 769, 110

Kahler, S. W., & Reames, D. V. 2003, ApJ, 584, 1063

Kahler, S. W., & Vourlidas, A. 2013, ApJ, 769, 143

Kahler, S. W., & Vourlidas, A. 2014, ApJ, in press

Kahler, S. W., Tylka, A. J., & Reames, D. V. 2009, ApJ, 701, 561

Kahler, S. W., Arge, C. N., Akiyama, S., & Gopalswamy, N. 2014, Sol. Phys., 289, 657

Kelly, J., Dalla, S., & Laitinen, T. 2012, ApJ, 750, 47

Laitinen, T., Dalla, S., & Marsh, M. S. 2013, ApJ, 773, L29

Lario, D., Aran, A., Gómez-Herrero, R., Dresing, N., Heber, B., Ho, G. C., Decker, R. B., & Roelof, E. C. 2013, ApJ, 767, 41

Mason, G. M., & Gloeckler, G. 2012, Space Sci. Rev., 172, 241

Mason, G. M., Desai, M. I., Mazur, J. E., & Dwyer, J. R. 2005, in The Physics of Collisionless Shocks, ed. G. Li, et al., AIP Conf. Proc. 781, 219

Mason, G. M., Desai, M. I., Mewaldt, R. A., & Cohen, C. M. S. 2013, in Centenary Symposium 2012: Discovery of Cosmic Rays, AIP Conf. Proc. 1516, 117

Mewaldt, R. A., Cohen, C. M. S., & Mason, G. M. 2006, in Solar Eruptions and Energetic Particles, ed. N. Gopalswamy et al., AGU Geophys. Mon. Series 165, 115

Mewaldt, R. A., Cohen, C. M. S., Mason, G. M., Cummings, A. C., Desai, M. I., Leske, R. A., Raines, J., Stone, E. C., Wiedenbeck, M. E., von Rosenvinge, T. T., & Zurbuchen, T. H. 2007, Space Sci. Rev., 130, 207

Mewaldt, R. A., Mason, G. M., Cohen, C. M. S., Gómez-Herrero, R., Haggerty, D. K., Leske, R. A., & Wiedenbeck, M. E. 2012a, in Physics of the Heliosphere: A 10 Year Perspective, AIP Conf. Proc. 1436, 206

Mewaldt, R. A., Mason, G. M., & Cohen, C. M. S. 2012b, in Space Weather: the Space Radiation Environment, ed. Q. Hu et al., AIP Conf. Proc. 1500, 128

Mewaldt, R. A., Cohen, C. M. S., Mason, G. M., von Rosenvinge, T. T., Leske, R. A., Luhmann, J. G., Odstrcil, D., & Vourlidas, A. 2013, in Solar Wind 13, AIP Conf. Proc. 1539, 116

Miteva, R., Klein, K.-L., Malandraki, O., & Dorrian, G. 2013, Sol. Phys., 282, 579

Ragot, B. R. 2011, ApJ, 740, 119

Ragot, B. R. 2012, ApJ, 758, 89

Reames, D. V. 2013, Space Sci. Rev., 175, 53

Reinard, A. A., Lynch, B. J., & Mulligan, T. 2012, ApJ, 761:175

Richardson, I. G. 2013, private communication

Richardson, I. G., & Cane, H. V. 2010, Sol. Phys., 264, 189

Richardson, I. G., & Cane, H. V. 2012, J. Space Weather Space Climate., 2, A02

Ruzmaikin, A., Feynman, J., & Stoev, S. A. 2011, J. Geophys. Res., 116, A04220

Tylka, A. J., & Lee, M. A. 2006, ApJ, 646, 1319

Zurbuchen, T. H., & Richardson, I. G. 2006, Space Sci. Rev., 123, 31

This 2-column preprint was prepared with the AAS LaTeX macros v5.2.

Table 1: SEP Event Median Values for the Different SW Types.

SEP Parameter	SW 1	SW 2	SW 3	SW 2+3	St Dev
Event numbers	34	28	34	62	
TO (hrs)	1.85	1.70	1.75	1.75	1.77
TR (hrs)	2.50	1.50	2.25	1.50	2.72
TO+TR (hrs)	4.45	3.30	4.60	4.20	3.47
Lg 20 MeV p Ip	–0.52	–1.52	–1.52	–1.52	1.34
Lg 2 MeV p bgd	0.18	–0.42	–1.20	–0.71	1.25
Lg (Ip/bgd) R1	–1.09	–1.11	–0.54	–0.67	1.23
CME V(cdaw)	1405	1138	1186	1186	619
CME V(fr)	1334	1061	1170	1084	611
CME CDAW W	241°	188°	212°	197°	
Solar Longitude[a]	W76°	W72°	W90°	W90°	

[a] All events are west of W40°

Table 2: Correlation Coefficients CC between the SEP Event and CME Parameters for Different Solar Wind Types.

Parameters		SW 1	SW 2	SW 3	SW 2+3
Lg 20 MeV Ip	Lg 2 MeV bkd	0.60	0.46	0.50	0.45
Lg 20 MeV Ip	Lg V(cdaw)	0.74	0.18	0.50	0.36
R1	Lg V(cdaw)	0.17	0.30	0.24	0.25
Lg 2-MeV bkd	Lg V(cdaw)	0.73	–0.13	0.31	0.11

Table 3: Median Values of Transient SW Groups.

Parameter	MC	QuasiMC	Other
Event Numbers	8	10	16
Lg20 MeV	–2.06	0.10	–0.41
Lg2 MeVBkgd	–0.04	–0.01	0.61
R1	–1.44	–0.77	–1.04
CME V(cdaw)	1013	1405	1490
Longitude	W59°	W70°	W84°

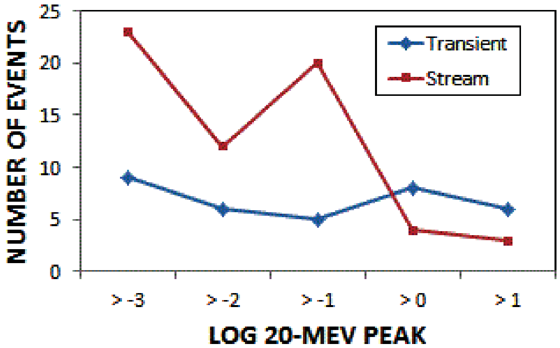

Fig. 1.— Number of 20-MeV SEP events in decadal bins of differential log Ip for the 34 events in type 1 transients (squares) and 62 events in types 2+3 long-lived streams (diamonds)

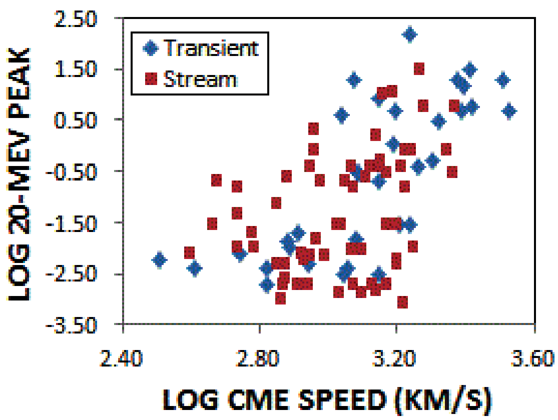

Fig. 2.— Log-log plot of 20 MeV SEP Ip versus the CME speed V(cdaw) for the SEP events in transient and long-lived stream SW types. The largest SEP events and CME speeds occur in the transient type 1 SW.

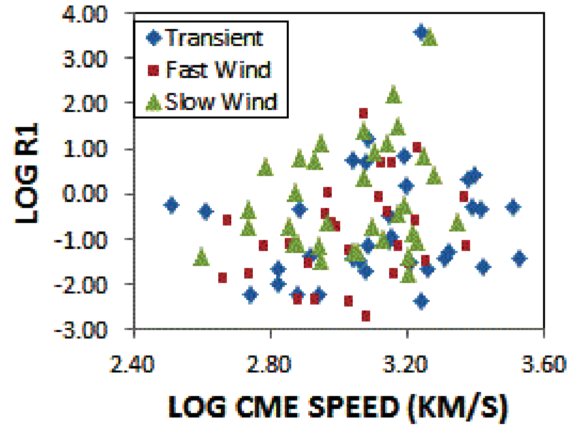

Fig. 3.— R1, the log of the 20-MeV event peak Ip normalized to the 2-MeV background, versus the logs of V(cdaw) for all three types of SW. The correlations are still positive, but much weaker than in the log-log plots of Ip versus V(fr) of Figure 2.

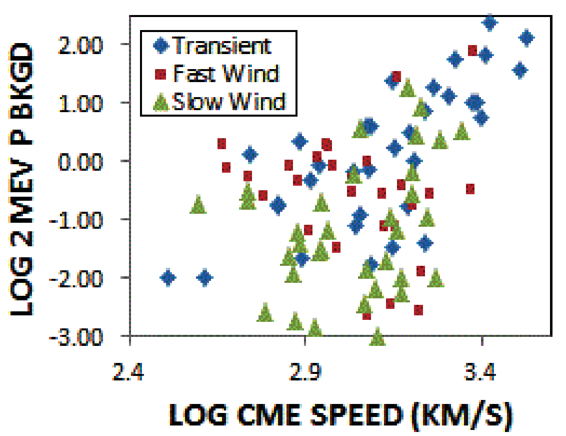

Fig. 4.— Log-log plot of the 2-MeV p background versus the CME V(cdaw) for the three SW types.

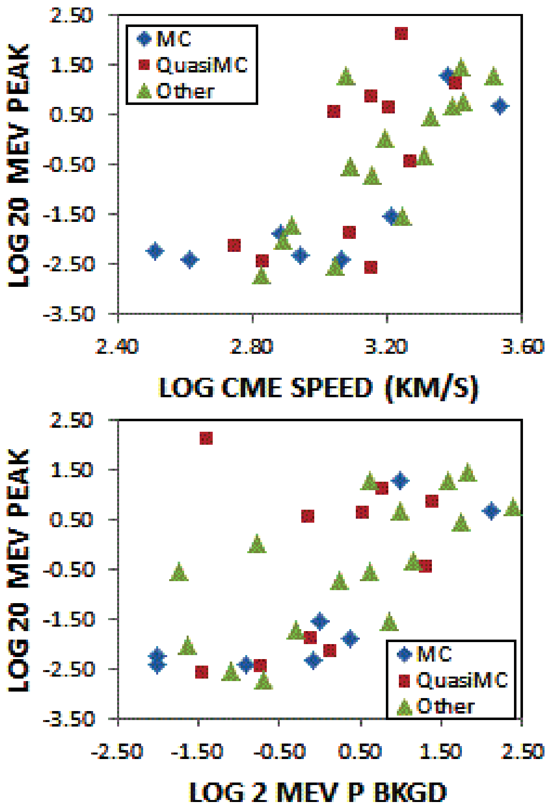

Fig. 5.— Log-log plot of Ip versus V(cdaw) (top) and 2-Mev background (bottom) for the type 1 SW SEP events of Figure 2. There are only 2 large MC events, those of 21 April 2002 and 10 November 2004.

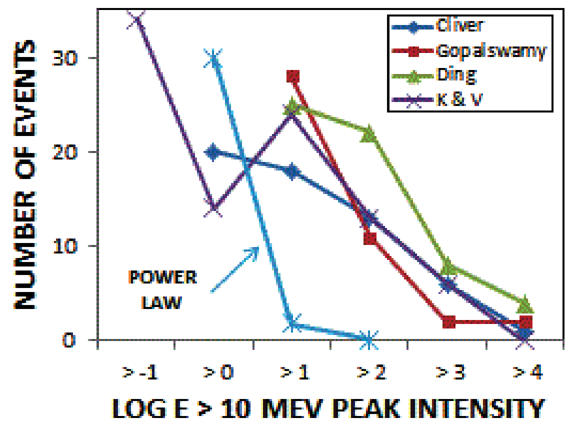

Fig. 6.— Linear-log plot of the distributions of differential peak intensities of $E > 10$ MeV SEP events from selected studies. A comparison power-law distribution with $\gamma = -1.22$ shown by asterisks would extend to 498 events in the > -1 bin and is 0.11 in the > 2 bin. The size distribution for this (K&V) study is converted from 20-MeV differential energy intensities to the $E > 10$ MeV intensities by assuming log $(E > 10$ MeV$)$ = log (20 MeV) + 1.8.